Ann Dermatol. 2024 Feb;36(1):18-28
https://doi.org/10.5021/ad.23.010
pISSN 1013-9087·eISSN 2005-3894

AD ANNALS of DERMATOLOGY

Original Article

Check for updates

Actinidia polygama Water Extract (APWE) Protects Against UVB-Induced Photoaging via MAPK/AP-1 and TGFβ-Smad Pathway

Jung Min Lee [1,2,*], **Su-Jin Park** [3,*], **Yu-jin Kim** [1,2], **Su-Young Kim** [1], **Yoo-na Jang** [1,2], **A yeon Park** [1,2], **Seong-Hyun Ho** [3], **Dayoung Kim** [3], **Jung Ok Lee** [1], **Kwang-Ho Yoo** [1], **Beom Joon Kim** [1,2]

[1]Department of Dermatology, College of Medicine, Chung-Ang University, Seoul, Korea
[2]Department of Medicine, Graduate School, Chung-Ang University, Seoul, Korea
[3]R&D Center, G&P Bioscience Co., Ltd., Seoul, Korea

OPEN ACCESS

Received: Feb 16, 2023
Revised: Jul 14, 2023
Accepted: Jul 14, 2023
Published online: Dec 20, 2023

Corresponding Author:
Beom Joon Kim
Department of Dermatology, College of Medicine, Chung-Ang University, 84 Heukseok-ro, Dongjak-gu, Seoul 06974, Korea.
Email: beomjoon74@gmail.com

*Jung Min Lee and Su-Jin Park contributed equally to the study.

ABSTRACT

Background: *Actinidia polygama* (silver vine) has been used in oriental medicine to treat gout, rheumatoid arthritis, and inflammation. *Actinidia polygama* water extract (APWE) is named PB203.
Objective: To investigate whether PB203 has anti-photoaging effects and to understand the molecular mechanism underlying such effects.
Methods: The antioxidant effect was assessed by 1,1-diphenyl-2-picrylhydrazyl assay and 2′,7′-dichlorodihydrofluorescein diacetate staining in ultraviolet B (UVB)-irradiated HaCaT cells with or without PB203 treatment. Type I collagen, matrix metalloproteinase-1 (MMP-1), tissue inhibitor of metalloproteinase (TIMP-1), hyaluronic acid (HA), hyaluronan synthase 1 (HAS1) and HAS2 levels were measuring by enzyme-linked immunosorbent assay or reverse transcription quantitative polymerase chain reaction. Also, we investigate the effects of PB203 on wrinkle formation, and the potential mechanisms underlying such effects were investigated in UVB-induced wrinkle mouse model mice.
Results: PB203 alleviated the UVB-induced reactive oxygen species production, phosphorylation of JNK, ERK, and p38, and formation of AP-1. In addition, PB203 inhibited the decreases in type I collagen and TIMP-1 levels, and the increase in MMP-1 levels in UVB-exposed HaCaT cells. In UVB-induced wrinkle mouse model, PB203 inhibited the decreases in elastin and type I collagen levels as well as the increases in MMP-1 expression, wrinkle formation, and skin dehydration. Furthermore, PB203 increased the expression of filaggrin, HAS1, and HAS2, improving the skin barrier function.
Conclusion: Taken together, we found that PB203 is as a potent candidate to serve as a functional ingredient or therapeutic agent to improve UVB-mediated skin aging.

Keywords: Antioxidants; Reactive oxygen species; Skin aging; Ultraviolet rays

INTRODUCTION

Ultraviolet radiation (UVR) is critical factor for skin aging[1]. UV-mediated skin aging, such as wrinkles, are closely related to altered expression of matrix metalloproteinases (MMPs) and type I collagen[2,3]. Reactive oxygen species (ROS) are produced during UVR[1]. An increase in ROS levels leads to the disruption of cellular homeostasis, accumulation of oxidative stress, and a reduction in the expression of antioxidant enzymes[4]. ROS also activate the mitogen-activated protein kinase (MAPK) signaling pathway leading

to an increase in the expression and phosphorylation of c-Jun and c-Fos, forming the transcription factor complex, activator protein-1 (AP-1)[4]. AP-1 upregulates the expression of MMPs[4], which degrade collagen and other extracellular matrix proteins that form the dermal connective tissue, promoting wrinkle formation and skin aging[5].

UVR inhibits type I collagen production by suppressing transforming growth factor β (TGFβ)-Smad signaling pathway. TGFβ binds to TGFβ type II receptor (TβRII) and recruits TGFβ type I receptor (TβRI), forming a heterotetrametric complex. This complex formation results in the phosphorylation of TβRI by TβRII kinase, and p-TβRI phosphorylates the receptor-activated Smads (R-SMADs) Smad2 and Smad3, resulting in the formation of hetero-oligomers with the common mediator, Smad4. The hetero-oligomers translocate from the cytoplasm to the nucleus, where they regulate the transcription of target genes, including type I collagen6,7. Accordingly, UVR induces wrinkles and skin aging via the ROS-MAPK/AP-1/TGFβ-Smad signaling cascade.

Filaggrin involved in the terminal differentiation of keratinocytes, the function of the skin barrier, and the formation of the stratum corneum (SC)8. The SC is the first line of defense against UVR, and a decrease in filaggrin levels by ultraviolet B (UVB) exposure leads to morphological changes in the SC lipids, transepidermal water loss (TEWL), and dehydration of the SC9.

In the previous study, we found that the use of water, instead of ethanol, for the extraction of *Actinidia polygama* (silver vine) does not affect its anti-photoaging effect[10]. Water can be used to dissolve a wide range of molecules due to its polarity and ability to form hydrogen bonds[11]. In addition, it is a safe, inexpensive, and eco-friendly. Therefore, water was selected as the extraction solvent for *A. polygama*, which has been used to relieve pain, gout, rheumatoid arthritis, and inflammation in traditional eastern medicinal practices[12,13]. We previously found that *A. polygama* extract had an anti-wrinkle and hydrating effect on UVB-irradiated hairless mice[10]. However, studies on the mechanism of this anti-wrinkle action have been lacking. Therefore, we analyzed the mechanisms underlying the protective effect of PB203 (*Actinidia polygama* water extract [APWE] is named PB203) against UVB both *in vitro* and *in vivo*.

MATERIALS AND METHODS

Preparation of PB203

To obtain PB203, i.e., the water extract powder of *A. polygama*, dried fruits of the plant were washed and extracted using water (water-to-fruit volume ratio, 14) at 85°C±5°C for 6±2 hours. The extracts were filtered and concentrated using a vacuum evaporator at 60°C. The concentrates were mixed with 30% dextrin (solid content 70% weight ratio) and powdered using a spray dryer. The dosage of PB203 used in this experiment was calculated as the solid content of the powdered extract.

Cell culture and UVB irradiation

HaCaT cells (ATCC) were cultured in Dulbecco's Modified Eagle Medium (DMEM) containing 10% fetal bovine serum (FBS; Hyclone, Logan, UT, USA) and 1% penicillin/streptomycin at 37°C in a humidified incubator (5% CO_2). The experiments were performed using subcultured cells between the second and fourth. Based on the results of a preliminary study, the optimum dose of UVB irradiation was determined as 30 mJ/cm^2 and applied in this study.

Cell viability

Cells were treated with 0, 5, 10, 20, or 40 μg/ml of PB203 and incubated for 24 hours. Cell viability was analyzed using a WST-1 assay at 450 nm using a microplate spectrophotometer (SpectraMax 340; Molecular Devices, Inc., San Jose, CA, USA).

Total phenolic content

The total phenolic content of PB203 was determined using the Folin-Ciocâlteu method[14] with minor modifications. Gallic acid was used as the standard at concentrations of 0.016, 0.031, 0.063, 0.125, 0.25, and 0.5 mg/ml. As such, 50 μL Folin-Ciocâlteu reagent was added to 100 μL of extract, and the solution was mixed with 1.35 ml distilled water and 1 ml sodium carbonate solution (Na_2CO_3, 7% w/v). The mixture was allowed to react in dark for 2 hours at room temperature, followed by the absorbance measurement at 750 nm. The results were expressed as Gallic acid equivalents (GAE; milligrams of GAE per gram plant material).

1,1-Diphenyl-2-picrylhydrazyl (DPPH) scavenging activity

PB203 was dissolved in dimethyl sulfoxide (DMSO) and mixed with 195 μl of DPPH solution to obtain a final concentration of 120 μM. The reaction mixture was kept in dark for 30 minutes at room temperature, and the change in absorbance was measured at 517 nm.

DPPH Radical Scavenging Activity (%)=100–{(OD of Sample/OD of Control)×100}.

Intracellular ROS

2′,7′-Dichlorodihydrofluorescein diacetate (DCFH-DA; Sigma-Aldrich, St. Louis, MO, USA) was used to detect intracellular ROS. Fluorescence was observed by a fluorescence microscope (DMi8; Leica, Wetzlar, Germany).

Enzyme-linked immunosorbent assay (ELISA)

The supernatant was analyzed for type I collagen and hyaluronic acid (HA) content per the manufacturer's instructions using a Human Collagen I Alpha 1 ELISA kit (Novus Biologicals, Centennial,

CO, USA) or a Hyaluronan Quantikine ELISA kit (R&D Systems, Minneapolis, MN, USA).

Experimental animals and UVB irradiation

Six-week-old SKH-1 hairless female mice were purchased from Saeron Bio Inc. (Uiwang, Korea). The mice were acclimated for seven days under the following conditions: 23°C±2°C, 55%±10% humidity, 12-hour light/12-hour dark cycle. We used the ARRIVE checklists[15] and randomly distributed the mice into the treatment groups according to body weight. A total of 44 hairless mice were divided into the following 4 groups (11 mice per group): Control (saline), UVB + saline ("UVB-only" group), UVB + PB203 (50 mg/kg), and UVB + PB203 (100 mg/kg). Photoaging was induced by UVB irradiation using a BIO-SPECTRA (Vilber Lourmat, Collégien, France) for three months. The starting dose of UVB irradiation was 30 mJ/cm^2 for three weeks. The intensity of irradiation was gradually increased by 10 mJ/cm^2 per 3 weeks during 12 weeks. Immediately after each session of UVB irradiation, the extract (50 mg/kg or 100 mg/kg) or saline (200 μl) was administered orally to the mice six times a week for 12 weeks.

RNA extraction and reverse transcription quantitative polymerase chain reaction (RT-qPCR)

Total RNA was extracted using TRIzol Reagent (Invitrogen; Thermo Fisher Scientific, Inc., Waltham, MA, USA). PrimeScript™ RT Master Mix (Takara, Tokyo, Japan) was used to synthesize the cDNA. qPCR was performed using qPCR PreMIX SYBR Green (Enzynomics, Seoul, Korea) on a CFX96 thermocycler (Bio-Rad, Hercules, CA, USA). Gene expression levels were calculated using the ΔΔCT method and normalized to those of glyceraldehyde-3-phosphate dehydrogenase (GAPDH). The primers used for qPCR are listed in **Supplementary Table 1**.

Western blot analysis

Total protein were resolved on a 10% sodium dodecyl-sulfate polyacrylamide gel electrophoresis through electrophoresis and transferred to a nitrocellulose membrane (Amersham™; Cytiva, Marlborough, MA, USA). The membranes were blocked in 5% skim milk in Tris-buffered saline containing 0.1% Tween-20, probed overnight at 4°C with the antibodies: anti-phospho-p38 anti-p38, anti-phospho-c-Jun N-terminal kinases (JNK), anti-JNK, anti-phospho-extracellular signal-regulated kinase (ERK), ERK, phospho-c-Jun, c-Jun, phospho-smad2, phospho-c-Fos, c-Fos purchased from Cell Signaling Technology Inc. (Beverly, MA, USA), anti-TGF-β1 (Proteintech, Rosemont, IL, USA), smad2+smdad3 (Abcam, Cambridge, UK), and aβ-Actin (Santa Cruz Biotechnology, Inc., Dallas, TX, USA). The membranes were washed and incubated with horseradish peroxidase-conjugated anti-mouse (Vector Laboratories Inc., Newark, CA, USA) or anti-rabbit (Vector Laboratories Inc.) secondary antibodies. Immunodetection was performed using an Amersham ECL kit (GE Healthcare, Chicago, IL, USA).

Histological observation and immunohistochemistry

The dorsal skin was collected, fixed in 10% formalin, dehydrated in ethanol, embedded in paraffin, sectioned, and stained with hematoxylin and eosin (H&E), Masson's trichrome (MT), and Victoria blue (VB). Immunohistochemistry (IHC) was performed using antibodies for type I collagen, MMP-1, and filaggrin. The stained tissues were observed under an optical microscope (DM750; Leica).

Assessment of wrinkle formation and elasticity

Wrinkle formation was measured using three-dimensional (3D) fringe projections (Courage and Khazaka Electronic GmbH, Köln, Germany; GFMesstechnik GmbH, Berlin, Germany)[10] and analyzed using the PRIMOS^{lite} software. Skin roughness was calculated by Rmax. Skin elasticity was measured using a Cutometer MPA 580 (Courage and Khazaka Electronic GmbH). The values were analyzed using the Software Cutometer® MPA 580, and an R2 parameter was calculated to measure the overall elasticity of the skin.

Assessment of skin hydration

SC hydration was assessed using a Corneometer® CM 825 (Courage and Khazaka Electronic GmbH). TEWL was measured at 12 weeks using a Tewameter® TM 300 (Courage and Khazaka Electronic GmbH).

Statistical analysis

Data were analyzed using an unpaired one-way analysis of variance followed by a Bonferroni *post hoc* test on GraphPad Prism 7.0 (GraphPad Software Inc., San Diego, CA, USA). All experiments were repeated at least three times, and the differences with *p*-values lower than 0.05 were considered statistically significant.

Ethics statement

All animal experiments were conducted according to the Principles of Laboratory Animal Care prescribed by the National Institutes of Health (NIH, Bethesda, MD, USA) and were approved by the Chung-Ang University Institutional Animal Care and Use Committee (IACUC No. 20190081).

RESULTS

PB203 has antioxidant properties

PB203 exhibited no cytotoxicity at concentrations 5–20 μg/ml and

a low cytotoxicity at 40 μg/ml (**Fig. 1A**). Phenolic compounds have significant oxidation-reduction properties[16]. The total phenolic content of PB203 was 28.4±0.48 mg GAE/g, and the total phenolic content of positive control (ascorbic acid) was 131±1 mg GAE/g (**Table 1**). The DPPH radical scavenging activity of PB203 increased in a dose-dependent manner, and the scavenging activity of PB203 20–80 mg/ml was similar to that of ascorbic acid 200 μg/ml (**Fig. 1B**). The UVB-induced increase in dichlorofluorescein fluorescence intensity was reduced upon pretreatment with PB203 (10 and 20 μg/ml), suggesting that PB203 exhibits a protective effect against UVB through its antioxidant activity (**Fig. 1C**).

Table 1. Total polyphenol content in PB203

Sample	PB203	Ascorbic acid
Total polyphenols (mg GAE/g)	28.4±0.48	131±1

GAE: Gallic acid equivalents.

PB203 inhibits UVB-induced MMP-1 increase and collagen decrease by regulating MAPK/AP-1/TGFβ-Smad pathway in HaCaT cells

We measured the levels of type I collagen by ELISA and analyzed the mRNA levels of MMP-1 and tissue inhibitor of metalloproteinase-1 (TIMP-1) by RT-qPCR in UVB-irradiated HaCaT cells with or

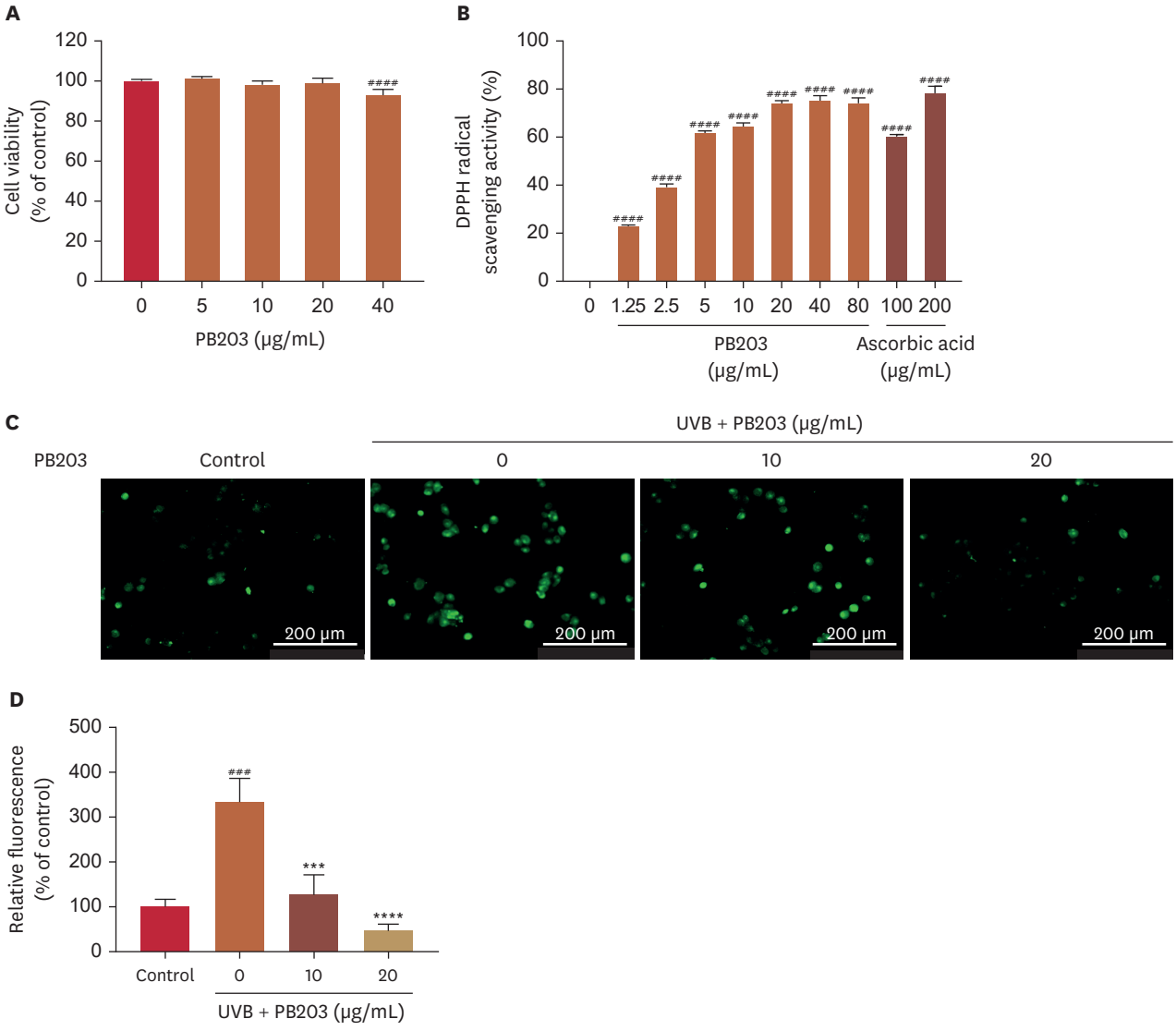

Fig. 1. The effect of PB203 on the viability and intracellular ROS levels of HaCaT cells. (A) Viability of HaCaT cells treated with PB203 (0, 5, 10, 20, and 40 μg/ml) for 24 hours. (B) DPPH radical scavenging activity of PB203, and ascorbic acid. (C, D) HaCaT cells were pretreated with PB203 for 3 hours before irradiation with UVB (30 mJ/cm^2). Then, the cells were exposed to DCFH-DA for 45 minutes. The images were acquired using a fluorescence microscope and quantified on ImageJ. The results are shown as the mean ± standard deviation.
ROS: reactive oxygen species, DPPH: 1,1-diphenyl-2-picrylhydrazyl, UVB: ultraviolet B, DCFH-DA: 2′,7′-dichlorodihydrofluorescein diacetate.
$^{###}p<0.001$, $^{####}p<0.0001$ compared with the control group; $^{***}p<0.001$, $^{****}p<0.0001$ compared with the UVB + media group.

https://doi.org/10.5021/ad.23.010

AD ANNALS of DERMATOLOGY

without PB203 treatment. PB203 ameliorated the UVB-induced decrease in type I collagen levels (**Fig. 2A**). PB203 also significantly prevented the UVB-induced increase in MMP-1 mRNA levels and reversed the decrease in TIMP-1 mRNA levels (**Fig. 2B and C**). Additionally, UVB exposure significantly increased the phosphorylation of MAPKs, including p38, JNK, and ERK. In contrast, pretreatment with PB203 suppressed the UVB-induced phosphorylation of p38, JNK, and ERK in a dose-dependent manner (**Fig. 2D**). UVB exposure increased the phosphorylation of both c-Jun and c-Fos. However, pretreatment with PB203 inhibited the phosphorylation of these proteins (**Fig. 2E**). UVB irradiation decreased TGF-β1 expression and the phosphorylation of Smad2 to 26.9% and 24.9%, respectively (**Fig. 2F**). PB203 (10 and 20 μg/ml), however, blocked the UVB-mediated TGFβ/Smad pathway inhibition. These findings demonstrate that PB203 inhibits the downregulation of collagen via the MAPK/AP-1 and TGFβ-Smad pathways in UVB-irradiated HaCaT cells.

PB203 suppresses UVB-induced decreases in HA, HAS1, HAS2, and filaggrin expression

HA is the main factor involved in skin moisture and has a unique capacity to retain water[17]. Treatment with PB203 increased HA levels in a dose-dependent manner (**Fig. 3A**). HAS synthesizes HA and plays a key role in regulating HA levels[18]. HAS1 and HAS2 mRNA levels in UVB-irradiated HaCaT cells (with and without PB203 treatment) were analyzed by a RT-qPCR. UVB irradiation reduced the mRNA levels of HAS1 and HAS2; PB203 treatment rescued the UVB-induced decreases in HAS1 and HAS2 mRNA

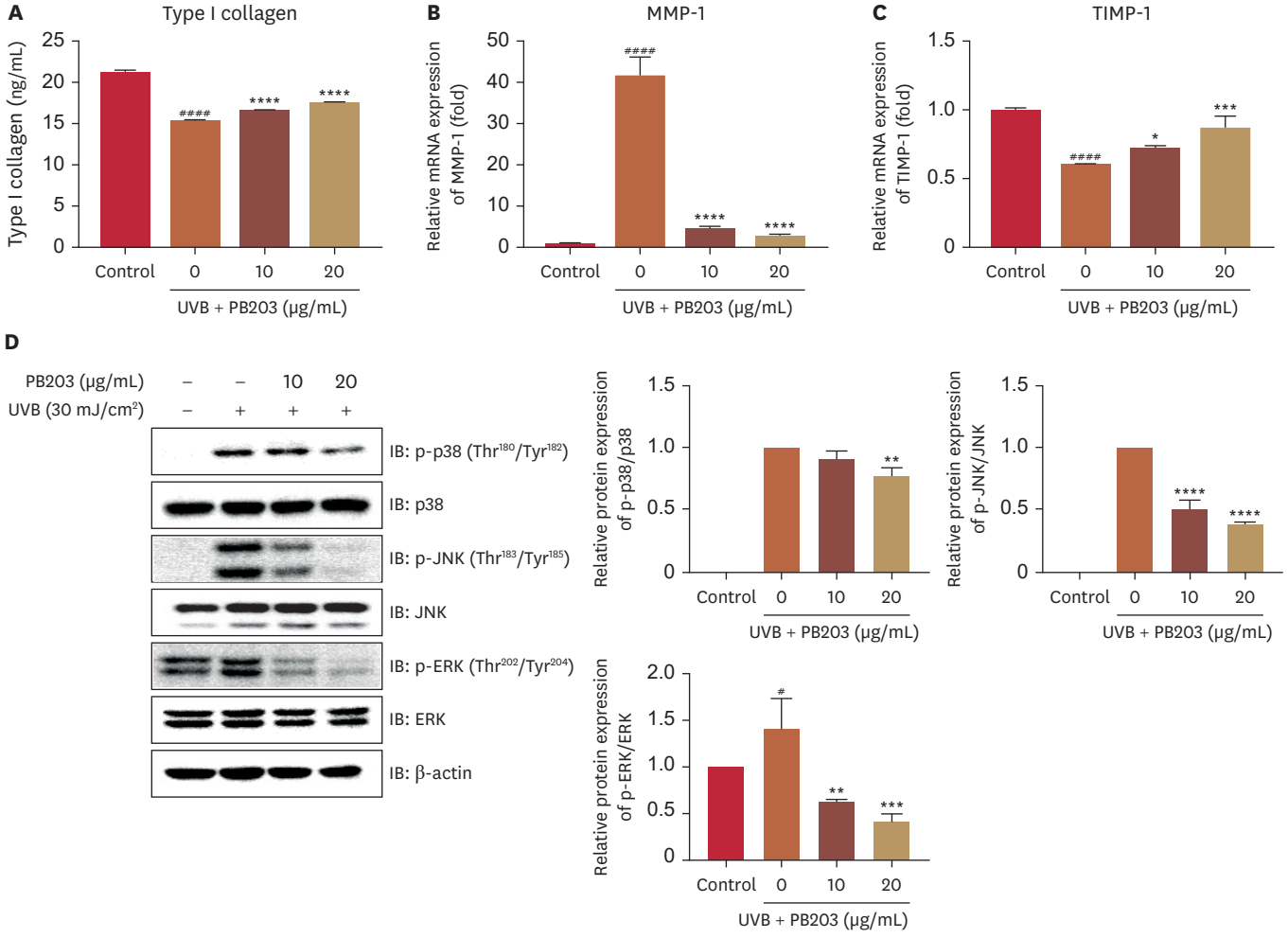

Fig. 2. PB203 prevents the inhibition of type I collagen, MMP-1, TIMP-1, MAPK, AP-1, and TGFβ signaling pathway after UVB exposure. (A) Type I collagen levels. (B, C) The mRNA expression levels of MMP-1 and TIMP-1. (D) Total and phosphorylated protein levels of p38, JNK, and ERK. (E) Total and phosphorylated protein levels of c-Jun and c-Fos. (F) The levels of TGF-β1, p-Smad2, and Smad2/3.
The values are shown as the mean ± standard deviation.
MMP: matrix metalloproteinase, TIMP: tissue inhibitor of metalloproteinase-1, MAPK: mitogen-activated protein kinase, AP-1: activator protein-1, TGF: transforming growth factor, UVB: ultraviolet B, JNK: c-Jun N-terminal kinases, ERK: extracellular signal-regulated kinase.
$^{\#}p<0.05$, $^{\#\#\#}p<0.001$, $^{\#\#\#\#}p<0.0001$ compared with the control group; $^{*}p<0.05$, $^{**}p<0.01$, $^{***}p<0.001$, $^{****}p<0.0001$ compared with the UVB + media group.

(continued to the next page)

https://doi.org/10.5021/ad.23.010

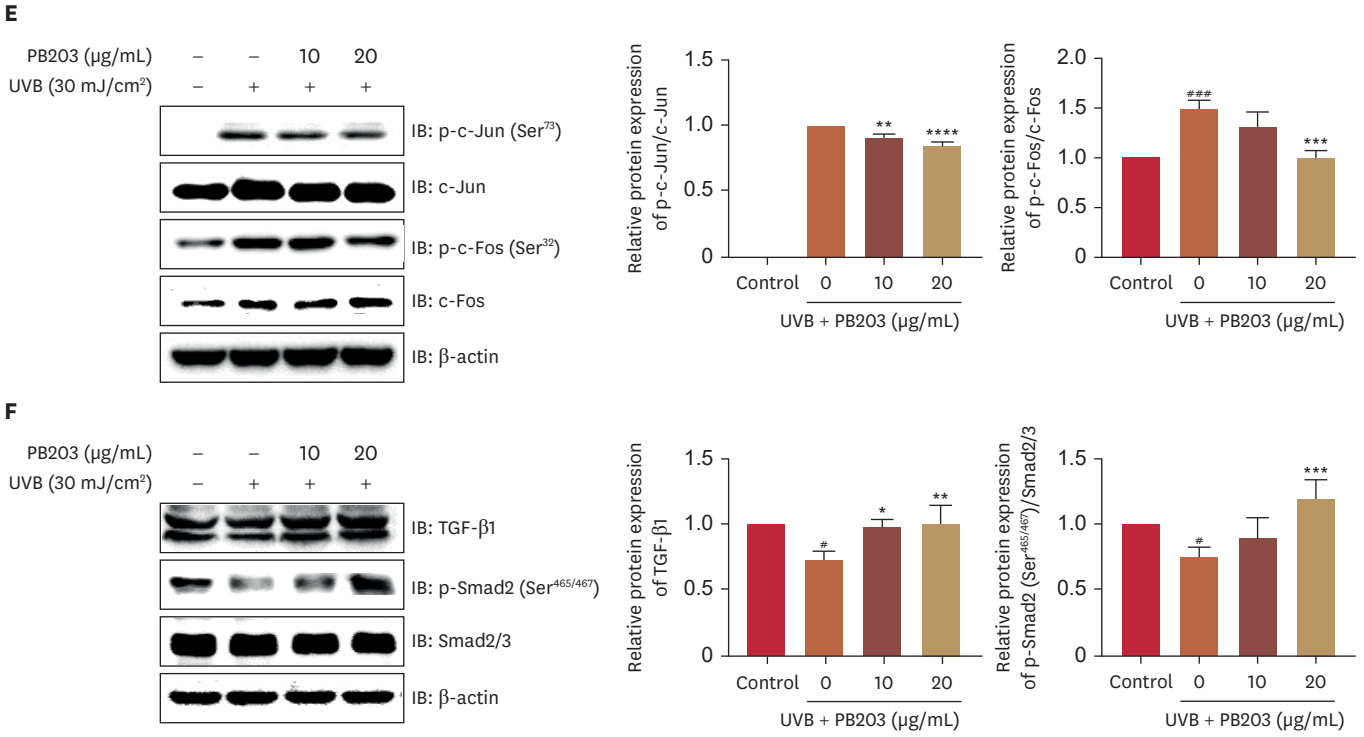

Fig. 2. (Continued) PB203 prevents the inhibition of type I collagen, MMP-1, TIMP-1, MAPK, AP-1, and TGFβ signaling pathway after UVB exposure. (A) Type I collagen levels. (B, C) The mRNA expression levels of MMP-1 and TIMP-1. (D) Total and phosphorylated protein levels of p38, JNK, and ERK. (E) Total and phosphorylated protein levels of c-Jun and c-Fos. (F) The levels of TGF-β1, p-Smad2, and Smad2/3.
The values are shown as the mean ± standard deviation.
MMP: matrix metalloproteinase, TIMP: tissue inhibitor of metalloproteinase-1, MAPK: mitogen-activated protein kinase, AP-1: activator protein-1, TGF: transforming growth factor, UVB: ultraviolet B, JNK: c-Jun N-terminal kinases, ERK: extracellular signal-regulated kinase.
$^{\#}p<0.05$, $^{\#\#\#}p<0.001$, $^{\#\#\#\#}p<0.0001$ compared with the control group; $^{*}p<0.05$, $^{**}p<0.01$, $^{***}p<0.001$, $^{****}p<0.0001$ compared with the UVB + media group.

levels (**Fig. 3B and C**). After UVB irradiation, filaggrin levels decreased by 34.4% compared to the control group; however, treatment with PB203 (20 μg/ml) increased filaggrin levels by 41.4% compared to the UVB + media group (**Fig. 3D**). Overall, these results indicate that UVB irradiation leads to a decrease in the function of the skin barrier, and PB203 protects the barrier function from UVB-mediated damage by improving skin hydration.

Oral administration of PB203 reduces UVB-induced wrinkle formation

The schematic diagram of animal experiments is shown in **Fig. 4A**. The body weights of the mice did not significantly differ after 12 weeks of PB203 or UVB treatment, indicating that PB203 and UVB treatments were safe (**Fig. 4B**). We examined if PB203 prevents wrinkle formation in UVB-irradiated hairless mice. A visual assessment showed that oral administration of PB203 reduced UVB-induced wrinkles (**Fig. 4C**). Roughness Rmax values in the UVB-irradiated group were significantly higher than those in the non-irradiated control group. UVB-exposed mice administrated with PB203 (50 mg/kg or 100 mg/kg) exhibited a reduction in the maximum wrinkle area compared to mice irradiated with UVB but not received PB203 (**Fig. 4F**). The thickness of epidermis was approximately 4.6-fold higher in the UVB-irradiated group than in the control group; however, it was significantly reduced in UVB-irradiated mice treated with PB203 (50 or 100 mg/kg) compared with the UVB-only group (**Fig. 4D and G**). In addition, oral administration of PB203 (50 or 100 mg/kg) suppressed the loss of elasticity in the dorsal skin of UVB-exposed mice in a dose-dependent manner (**Fig. 4E and H**).

PB203 suppresses UVB-induced collagen degradation by down-regulating MMP-1 and improves skin hydration

The collagen fiber content decreased after UVB irradiation, but treatment with PB203 (50 or 100 mg/kg) prevented this decrease, maintaining collagen fiber content at levels comparable to those in control mice (**Fig. 5A and E**). In addition, UVB-mediated decrease in type I collagen levels was inhibited by PB203 treatment (**Fig. 5B**). To understand how PB203 inhibits UVB-induced collagen degradation and wrinkle formation, we examined MMP-1 expression by IHC and western blot. UVB-induced MMP-1 expression decreased upon PB203 pretreatment (**Fig. 5C**). While the

ANNALS of DERMATOLOGY

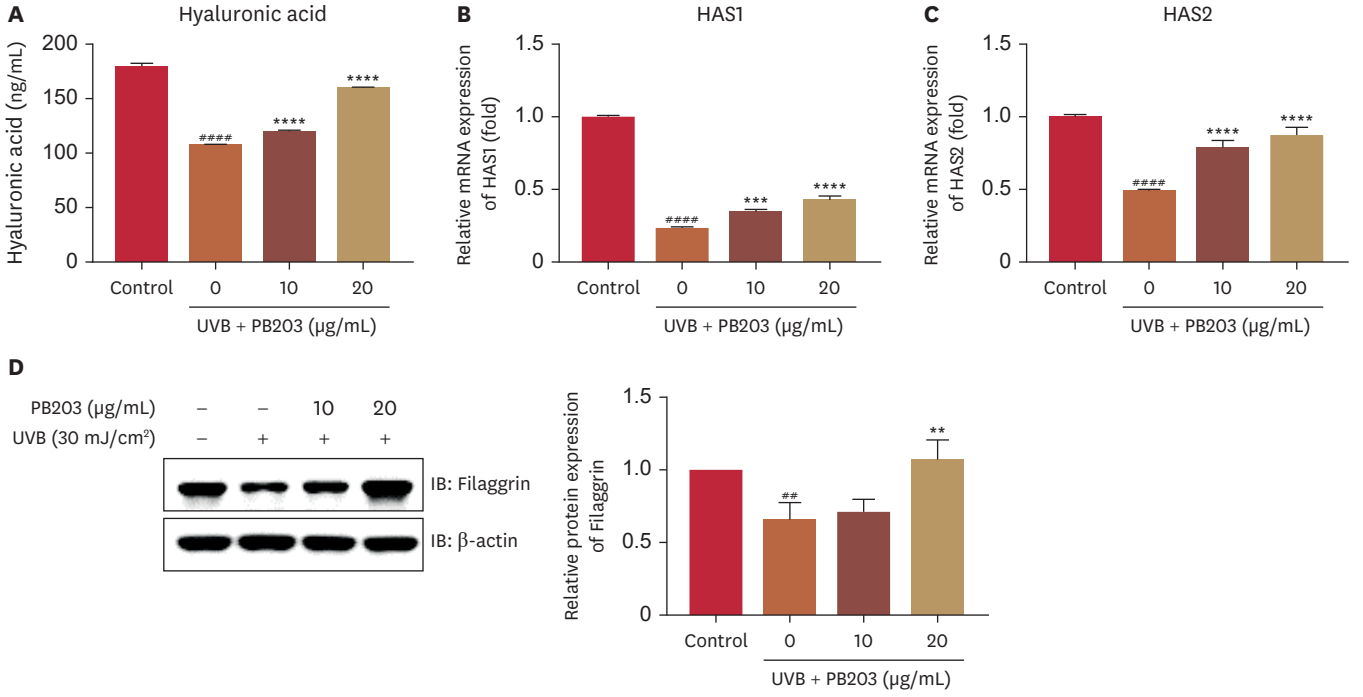

Fig. 3. PB203 prevents the UVB-induced downregulation of HA, HAS1, HAS2, and filaggrin. (A) The levels of HA. (B, C) The mRNA expression levels of HAS1 and HAS2. (D) The expression levels of filaggrin. The results are shown as the mean ± standard deviation.
HA: hyaluronic acid, HAS: hyaluronan synthase, UVB: ultraviolet B.
$^{\#\#}p<0.01$, $^{\#\#\#\#}p<0.0001$ compared with the control group; $^{**}p<0.01$, $^{***}p<0.001$, $^{****}p<0.0001$ compared with the UVB + media group.

UVB-only group exhibited a 2.9-fold increase in MMP-1 levels, PB203 (oral administration; 50 and 100 mg/kg) groups showed 1.7-fold (50 mg/kg) and 2.5-fold (100 mg/kg) decreases compared to the UVB-only group (**Fig. 5F**). Filaggrin levels were reduced in UVB irradiated mice but not in PB203-administrated mice (**Fig. 5D**). UVR leads to skin dehydration19. Skin hydration levels in the UVB-only group decreased by 38.9% compared with the control group (**Fig. 5G**). However, skin hydration increased by 21.2% and 22% in the PB203 groups receiving 50 and 100 mg/kg/day PB203, respectively, compared with the UVB-only group. In contrast, TEWL levels in the UVB-only group increased by 123.4% compared with the non-irradiated group, but those in mice treated with 50 and 100 mg/kg/day PB203 decreased by 108.1% and 115.8%, respectively, compared with the UVB-only group (**Fig. 5H**). In addition, the down-regulation of HAS1 and HAS2 due UVB irradiation was significantly prevented by PB203 treatment (**Fig. 5I and J**). Taken together, these results demonstrate that PB203 protects the skin against UVB irradiation by regulating the expression of collagen, MMP-1, HAS1, HAS2, and filaggrin.

DISCUSSION

PB203 quenched various adverse effects of UVR and provided photoprotective effects in UVB-irradiated HaCaT cells and hairless mice. *A. polygama* contains sugar, starch, protein, tannin, organic acid, and vitamins C, A, and flavonoids[20]. These compounds have been known to be important for physiological functions, including anti-oxidation and anti-inflammation[21,22]. In addition, it helps treat metabolic diseases, including obesity and hyperlipidemia, without side effects[23].

The extraction of natural materials is a important process for obtaining pure antioxidants from plants[24]. The using of solvent-free method has been of great interest as it reduce the cost and decrease the risks mediated with using organic solvents, increase production efficiency, and enhance safety[25]. In a previous study, no difference was detected between the anti-wrinkle effect of *A. polygama* extracted with water and ethanol[10]. Considering these findings and the economic benefits such as manufacturing cost and yield, water extraction was selected as the method of PB203 extraction from *A. polygama* fruits.

Natural antioxidants are classified into three main classes: polyphenolic compounds, vitamins, and carotenoids[26,27]. These natural antioxidants exhibit a wide range of biological effects, including anti-inflammatory, anti-aging, anti-atherosclerosis, and anticancer effects. The DPPH scavenging ability of PB203 increased in a dose-dependent manner (**Fig. 1B**). The DCFH-DA assay results further indicated that PB203 mitigated ROS-induced

https://doi.org/10.5021/ad.23.010

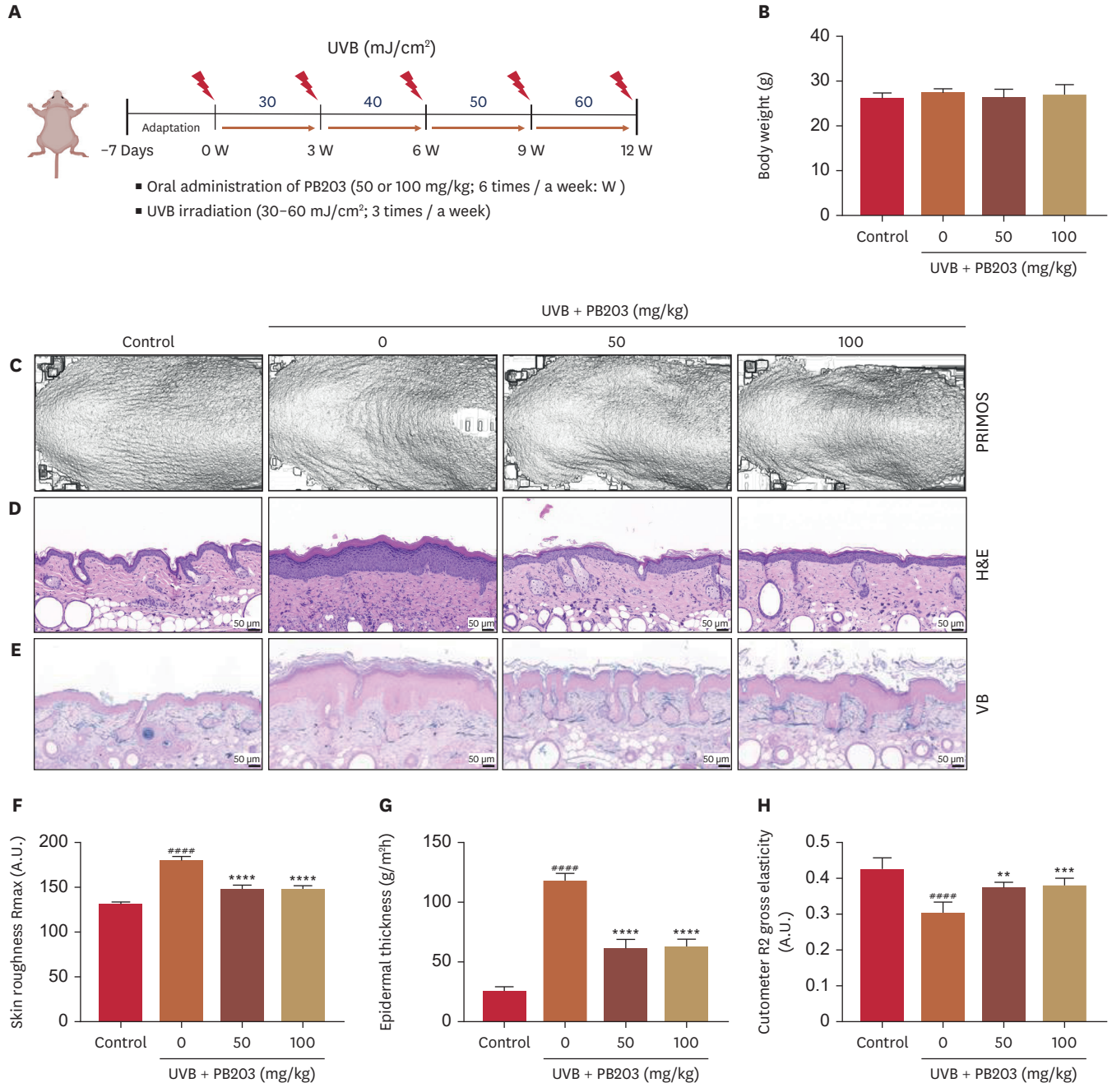

Fig. 4. PB203 inhibits UVB-induced wrinkle formation. (A) A schematic diagram of animal experiments. (B) Changes in body weight. (C-E) Images, H&E staining, and VB. Scale bar, 50 μm. (F) The quantification of wrinkles (roughness). (G) The epidermal thickness. (H) The gross elasticity (R2) of skin was measured using a Cutometer. Unit, skin roughness Rmax and cutometer R2 gross elasticity index (arbitrary unit). The results are shown as the mean ± standard deviation.
UVB: ultraviolet B, H&E: hematoxylin and eosin, VB: Victoria blue, Rmax: maximum roughness.
$^{\#\#\#\#}p<0.0001$ compared with the control group; $^{**}p<0.01$, $^{***}p<0.001$, $^{****}p<0.0001$ compared with the UVB + saline group.

damage to HaCaT cells by scavenging ROS (**Fig. 1C and D**). These results suggested that PB203 has a great potential as a natural antioxidant.

UVB-mediated MMPs increases were regulated by many signaling pathways and molecules including MAPK, AP-1, nuclear factor kappa B (NF-κB), and TGFβ/Smad[4]. UVB-induced ROS accumulation stimulated the phosphorylation of MAPKs that activate AP-1 and alter downstream gene expression. For example, following UV irradiation, p-JNK activates c-Jun, then p-c-Jun dimerizes with c-Fos, and this dimer forms an AP-1 complex to

https://doi.org/10.5021/ad.23.010

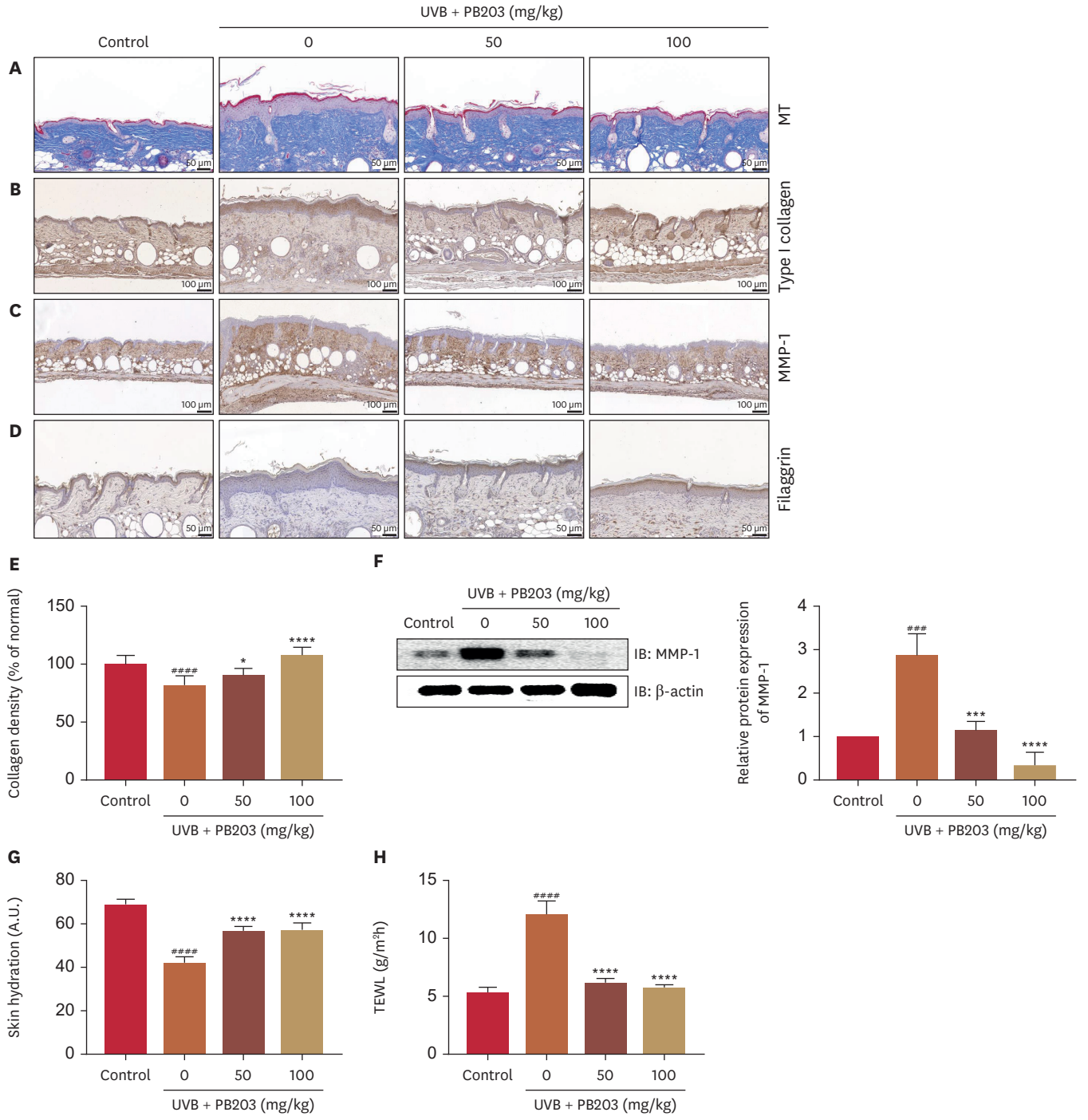

Fig. 5. The effect of oral administration of PB203 on the expression of type I collagen, MMP-1, filaggrin, HAS1, and HAS2. (A, E) MT staining and the collagen fiber levels were quantified using Image J. (B-D) Type I collagen, MMP-1, and filaggrin. (F) Expression of MMP-1 protein. (G) Skin hydration. (H) TEWL. (I, J) The mRNA levels of HAS1 and HAS2. The results are shown as the mean ± standard deviation.
MMP: matrix metalloproteinase; HAS: hyaluronan synthase, MT: Masson trichrome, TEWL: transepidermal water loss.
$^{###}p<0.001$, $^{####}p<0.0001$ compared with the control group; $^{*}p<0.05$, $^{***}p<0.001$, $^{****}p<0.0001$ compared with the UVB + saline group. (continued to the next page)

activate the expression of MMPs[4]. Similar to AP-1, NF-κB is an inflammation-related heterodimer consisting of p50 and p65 subunits involved in the regulation of MMP-1, MMP-3, and MMP-9 expression in photo-aging. Here, PB203 significantly downregulated the levels of p-c-Jun and p-c-Fos as well as those of p-p38, p-ERK, and p-JNK in UVB-irradiated HaCaT cells, resulting in a decrease in

https://doi.org/10.5021/ad.23.010

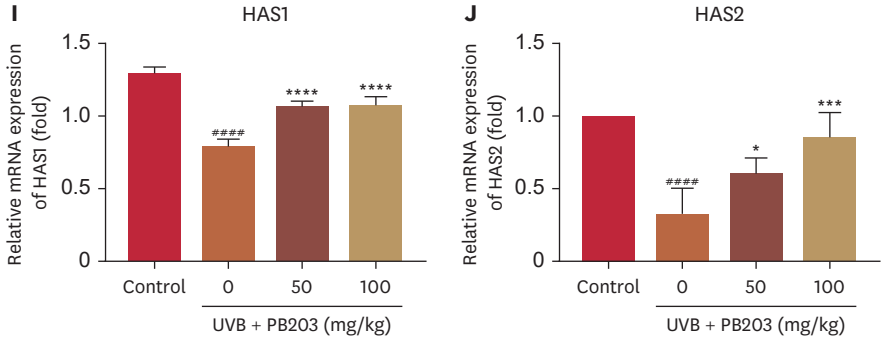

Fig. 5. (Continued) The effect of oral administration of PB203 on the expression of type I collagen, MMP-1, filaggrin, HAS1, and HAS2. (A, E) MT staining and the collagen fiber levels were quantified using Image J. (B-D) Type I collagen, MMP-1, and filaggrin. (F) Expression of MMP-1 protein. (G) Skin hydration. (H) TEWL. (I, J) The mRNA levels of HAS1 and HAS2. The results are shown as the mean ± standard deviation.
MMP: matrix metalloproteinase; HAS: hyaluronan synthase, MT: Masson trichrome, TEWL: transepidermal water loss.
###$p<0.001$, ####$p<0.0001$ compared with the control group; *$p<0.05$, ***$p<0.001$, ****$p<0.0001$ compared with the UVB + saline group.

MMP-1 expression (**Fig. 2D and E**). These results demonstrate that PB203 mitigates the expression of MMPs by inactivating the MAPK/AP-1 pathway. However, the effect of PB203 on NF-κB activation is not clear, and further studies are needed to clarify whether NF-κB is involved in the reduction of MMPs by PB203.

Next, we examined the molecular mechanisms of PB203 on regulating collagen. UVB irradiation stimulates collagen degradation by inhibiting the TGFβ/Smad pathway[6,7]. PB203 significantly increased TGF-β expression and activated Smad2, preventing the degradation of collagen by UVB-expose (**Fig. 2F**). Collectively, ROS is a main trigger for UVR-mediated skin damage, and the antioxidant properties of PB203 improve multiple cell signaling pathways such as, TGFβ/Smad pathway (collagen synthesis) and MAPK/AP-1 signaling pathway (MMP synthesis), resulting in a reduction in MMP levels and an increase in collagen content in UVB-induced photoaging[1,2,4,6,7].

Filaggrin is an essential structural protein for the development and maintenance of the skin barrier. Filaggrin deficiency can lead to destroy the external skin membrane, then to induce increasing the pH of the skin[28], and cause to immune related skin disease, such as atopic dermatitis, and psoriasis[29]. In this study, we found that UVB irradiation reduced filaggrin expression, while PB203 recovered UVB-mediated filaggrin decrease in HaCaT cells and in the epidermis of mice (**Figs. 3D** and **5D**), suggesting that PB203 improves skin barrier function via upregulating filaggrin. There are some limitations of this study, First, it does not include a positive control. Second, we applied PB203 while inducing wrinkles to examine its preventive effect, but it is also necessary to further investigate the treatment effect of PB203 after the formation of wrinkles. Taken together, PB203 can be considered as a functional food ingredient for alternative therapy to improve UV-mediated photoaging.

ORCID iDs
Jung Min Lee
https://orcid.org/0000-0002-4670-2521
Su-Jin Park
https://orcid.org/0000-0002-2693-3664
Yu-jin Kim
https://orcid.org/0000-0002-1247-2887
Su-Young Kim
https://orcid.org/0000-0002-3251-5813
Yoo-na Jang
https://orcid.org/0000-0002-0014-9783
A yeon Park
https://orcid.org/0000-0002-4667-8875
Seong-Hyun Ho
https://orcid.org/0000-0001-5471-0372
Dayoung Kim
https://orcid.org/0000-0002-0390-676X
Jung Ok Lee
https://orcid.org/0000-0002-0048-5322
Kwang-Ho Yoo
https://orcid.org/0000-0002-0137-6849
Beom Joon Kim
https://orcid.org/0000-0003-2320-7621

FUNDING SOURCE
This study was funded by the Technology Development Program (S2981854), funded by the Ministry of SMEs and Startups (MSS, Korea).

CONFLICTS OF INTEREST
The authors have nothing to disclose.

DATA SHARING STATEMENT
The data that support the findings of this study are available from the corresponding author, upon reasonable request.

SUPPLEMENTARY MATERIAL

Supplementary Table 1

Primer sequences used for the quantification of gene expression

REFERENCES

1. Kammeyer A, Luiten RM. Oxidation events and skin aging. Ageing Res Rev 2015;21:16-29. PUBMED | CROSSREF
2. Ricciotti E, FitzGerald GA. Prostaglandins and inflammation. Arterioscler Thromb Vasc Biol 2011;31:986-1000. PUBMED | CROSSREF
3. Pillai S, Oresajo C, Hayward J. Ultraviolet radiation and skin aging: roles of reactive oxygen species, inflammation and protease activation, and strategies for prevention of inflammation-induced matrix degradation - a review. Int J Cosmet Sci 2005;27:17-34. PUBMED | CROSSREF
4. Schieber M, Chandel NS. ROS function in redox signaling and oxidative stress. Curr Biol 2014;24:R453-R462. PUBMED | CROSSREF
5. Silvers AL, Bachelor MA, Bowden GT. The role of JNK and p38 MAPK activities in UVA-induced signaling pathways leading to AP-1 activation and c-Fos expression. Neoplasia 2003;5:319-329. PUBMED | CROSSREF
6. Chan CP, Lan WH, Chang MC, Chen YJ, Lan WC, Chang HH, et al. Effects of TGF-β s on the growth, collagen synthesis and collagen lattice contraction of human dental pulp fibroblasts in vitro. Arch Oral Biol 2005;50:469-479. PUBMED | CROSSREF
7. Nakao A, Afrakhte M, Morén A, Nakayama T, Christian JL, Heuchel R, et al. Identification of Smad7, a TGFbeta-inducible antagonist of TGF-β signalling. Nature 1997;389:631-635. PUBMED | CROSSREF
8. Kim Y, Lim KM. Skin barrier dysfunction and filaggrin. Arch Pharm Res 2021;44:36-48. PUBMED | CROSSREF
9. Lipsky ZW, German GK. Ultraviolet light degrades the mechanical and structural properties of human stratum corneum. J Mech Behav Biomed Mater 2019;100:103391. PUBMED | CROSSREF
10. Kim YJ, Lee JO, Kim SY, Lee JM, Lee E, Na J, et al. Effect of *A. polygama* APEE (*Actinidia polygama* ethanol extract) or APWE (*Actinidia polygama* water extract) on wrinkle formation in UVB-irradiated hairless mice. J Cosmet Dermatol 2023;22:311-319. PUBMED | CROSSREF
11. Brini E, Fennell CJ, Fernandez-Serra M, Hribar-Lee B, Lukšič M, Dill KA. How water's properties are encoded in its molecular structure and energies. Chem Rev 2017;117:12385-12414. PUBMED | CROSSREF
12. Lee YC, Kim SH, Seo YB, Roh SS, Lee JC. Inhibitory effects of Actinidia polygama extract and cyclosporine A on OVA-induced eosinophilia and bronchial hyperresponsiveness in a murine model of asthma. Int Immunopharmacol 2006;6:703-713. PUBMED | CROSSREF
13. Bang MH, Chae IG, Lee EJ, Baek NI, Baek YS, Lee DY, et al. Inhibitory effects of actinidiamide from *Actinidia polygama* on allergy and inflammation. Biosci Biotechnol Biochem 2012;76:289-293. PUBMED | CROSSREF
14. Folin O, Denis W. On phosphotungstic-phosphomolybdic compounds as color reagents. J Biol Chem 1912;12:239-243. CROSSREF
15. Percie du Sert N, Hurst V, Ahluwalia A, Alam S, Avey MT, Baker M, et al. The ARRIVE guidelines 2.0: updated guidelines for reporting animal research. PLoS Biol 2020;18:e3000410. PUBMED | CROSSREF
16. Soobrattee MA, Neergheen VS, Luximon-Ramma A, Aruoma OI, Bahorun T. Phenolics as potential antioxidant therapeutic agents: mechanism and actions. Mutat Res 2005;579:200-213. PUBMED | CROSSREF
17. Papakonstantinou E, Roth M, Karakiulakis G. Hyaluronic acid: a key molecule in skin aging. Dermatoendocrinol 2012;4:253-258. PUBMED | CROSSREF
18. Siiskonen H, Oikari S, Pasonen-Seppänen S, Rilla K. Hyaluronan synthase 1: a mysterious enzyme with unexpected functions. Front Immunol 2015;6:43. PUBMED | CROSSREF
19. Jariashvili K, Madhan B, Brodsky B, Kuchava A, Namicheishvili L, Metreveli N. UV damage of collagen: insights from model collagen peptides. Biopolymers 2012;97:189-198. PUBMED | CROSSREF
20. Park EJ. Quality characteristics of muffin added with *Actinidia polygama* powder. Culin Sci Hosp Res 2016;22:125-135. CROSSREF
21. Sashida Y, Ogawa K, Mori N, Yamanouchi T. Triterpenoids from the fruit galls of *Actinidia polygama*. Phytochemistry 1992;31:2801-2804. CROSSREF
22. Shoyama Y, Chen S, Tanaka H, Sasaki Y, Sashida Y. Actinidia polygama (Japanese name Matatabi): *in vitro* culture, micropropagation, and the production of monoterpenes and triterpenoids. In: Bajaj YPS, editor. Medicinal and Aromatic Plants X. New York: Springer Publishing, 1998: 1-13.
23. Sung YY, Yoon T, Yang WK, Moon BC, Kim HK. Anti-obesity effects of *Actinidia polygama* extract in mice with high-fat diet-induced obesity. Mol Med Rep 2013;7:396-400. PUBMED | CROSSREF
24. Xu DP, Li Y, Meng X, Zhou T, Zhou Y, Zheng J, et al. Natural antioxidants in foods and medicinal plants: extraction, assessment and resources. Int J Mol Sci 2017;18:96. PUBMED | CROSSREF
25. Chemat F, Abert Vian M, Ravi HK, Khadhraoui B, Hilali S, Perino S, et al. Review of alternative solvents for green extraction of food and natural products: panorama, principles, applications and prospects. Molecules 2019;24:3007. PUBMED | CROSSREF
26. Dorman H, Peltoketo A, Hiltunen R, Tikkanen M. Characterisation of the antioxidant properties of de-odourised aqueous extracts from selected Lamiaceae herbs. Food Chem 2003;83:255-262. CROSSREF
27. Sikora E, Cieślik E, Topolska K. The sources of natural antioxidants. Acta Sci Pol Technol Aliment 2008;7:5-17.
28. McAleer MA, Irvine AD. The multifunctional role of filaggrin in allergic skin disease. J Allergy Clin Immunol 2013;131:280-291. PUBMED | CROSSREF
29. Gruber R, Elias PM, Crumrine D, Lin TK, Brandner JM, Hachem JP, et al. Filaggrin genotype in ichthyosis vulgaris predicts abnormalities in epidermal structure and function. Am J Pathol 2011;178:2252-2263. PUBMED | CROSSREF